s-wave halo effect and the Coulomb barrier top effect on the mirror state of a halo

Shigeyoshi Aoyama
Information Processing Center, Kitami Institute of Technology, Kitami 090, Japan
(Received 25 October 1999; published 14 August 2000)

The Thomas-Ehrman shift for ^{11}Be and ^{11}N mirror nuclei, which was recently observed as a differential energy shift between *s* and other orbital states, is investigated in terms of complex expectation values. In calculating the complex expectation values, we use a new method which was recently proposed within the framework of the complex scaling method. The physical origin of the energy shift can be understood by considering the effects of the *s*-wave halo and the Coulomb barrier top. These two effects are discussed as another proof of a halo in addition to the observation of large matter radii in the drip-line nuclei.

PACS number(s): 21.10.Dr, 21.10.Sf, 25.70.Ef, 27.20.+n

I. INTRODUCTION

Recently, studies of neutron- and proton-drip-line nuclei have attracted much interest [1]. One of the most interesting subjects for studies of these drip-line nuclei is to understand differences between mirror states near to the drip-line. For example, a differential energy shift was recently observed in the mirror states of $^{11}_{7}$N and $^{11}_{4}$Be nuclei (see Fig. 1) [2,3]; the level spacings between the ground state and its excited states in ^{11}N becomes large in comparison with ones in ^{11}Be. The shifted ground state of ^{11}N is the mirror one of a famous halo state in ^{11}Be, which is known to be an *s*-wave halo of a valence neutron. The halo structure is interpreted as being a large cloud of extremely weakly bound valence neutrons around a core nucleus. Understanding the halo structure has been one of main subjects in the study of the drip-line nuclei.

Using several models, theoretical studies have been made for ^{11}N [4–7] to predict the ground-state energy. In these studies, the parameters for the nuclear potential are determined by fitting the energy levels of ^{11}Be. The predicted energy levels of ^{11}N are shown in Fig. 1. Due to the different assumptions concerning the *R*-matrix framework [5], the calculated energies are slightly different from each other, though our approach is based on the *S*-matrix framework. As shown in Fig. 1, all of the theoretical results show large differential energy shifts; thus the observed energy shift is theoretically reproduced. One of the mechanisms for this kind of the differential energy shift is known as the Thomas-Ehrman shift [8,9]. This shift has been systematically observed as a threshold effect for this past half century [10]. It is considered that the shift mainly arises from the difference in the Coulomb energy for each single-particle orbit [11]. However, the differential energy shift in the ^{11}Be-^{11}N mirror pair seems to be larger than the simple difference of the Coulomb energy. In the beginning of a study of drip-line nuclei, through systematic analyses of the Thomas-Ehrman shift, Comay *et al.* pointed out a puzzle: the energy shift shows an anomalous behavior beyond the proton-drip line [12], where further mechanisms for the energy shift would be required. This puzzle has not yet been solved, and now the large shift is also confirmed for ^{11}N beyond the proton-drip-line, which is mirror to a typical halo nucleus ^{11}Be on the neutron-drip-line. Therefore, it is meaningful to confirm the real mechanisms of the differential energy shift in the drip-line nuclei.

In a previous paper [7], to explain the Thomas-Ehrman shift in ^{11}Be and ^{11}N mirror nuclei, we discussed two comparable mechanisms that arise from the Coulomb interaction. One is the large Coulomb energy reduction for a halo orbit, the other is the energy shift originating from the Coulomb barrier top energy. However, it was not easy to separate the two mechanisms clearly at that time, since we could only calculate the complex energy-eigenvalue of the total Hamiltonian; the contribution for each term has not been discussed. On the other hand, if it is a resonance state with a narrow decay width, we know that the complex matrix element or the complex expectation value can be calculated by using several methods. However, in a practical calculation, it is not easy to obtain stable solutions for the resonance states with broad decay widths. For example, a difficulty in the convergent factor method is shown in Ref. [13]. Recently, Homma, Myo, and Kato proposed a simple method to calculate the complex matrix element or the complex expectation value based on the framework of the complex scaling method (CSM) [13]. CSM has been proved to be a useful

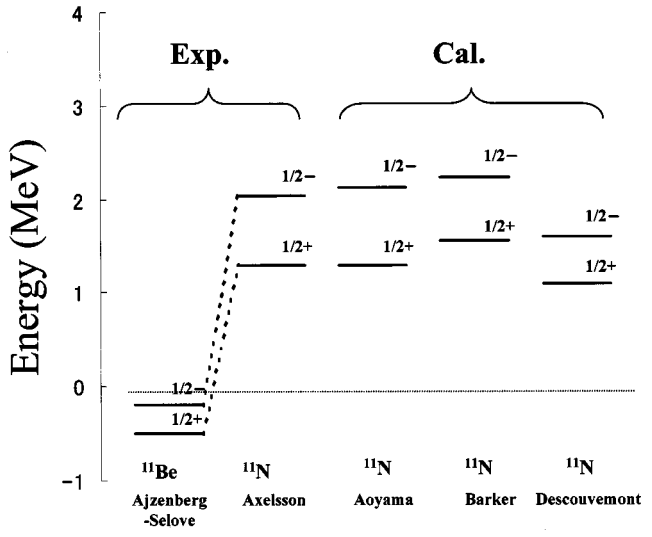

FIG. 1. Experimental energy levels for ^{11}Be [10] and ^{11}N [2], and calculated energy levels for ^{11}N [7,5,6].

method to study resonant structures, especially for unstable nuclei [14,15]. By applying this new method [13] to a simple potential model [16], we successfully explained two mechanisms of the anomalous energy shift related to the *s* wave: (i) the *s*-wave halo (Thomas-Ehrman) effect and (ii) the Coulomb barrier top effect. These two effects are discussed later in detail.

For an anomalous energy shift related to the *s* wave in drip-line nuclei, several groups also recently started analyses. For example, the effect of a change for the residual interaction in *s*-wave halo orbits has been discussed by Ogawa *et al.* [17]. Further, a change in the *s*-*d* coupling amplitude in the proton-rich side has been discussed [18], which means that the *s*-wave component in the core+*p* system becomes large compared to the mirror core+*n* one. In the present paper, we only discuss the *s*-wave halo effect and the Coulomb barrier top effect with a simple core+*N* model. However, the present two effects have a complementary large contribution to the energy shift. We thus expect that the present study gives a basis for the energy shift related to the *s* wave, though it should be discussed with a more developed model which includes all of the possible effects in the future.

In this paper, we explain two mechanisms: (i) the *s*-wave halo effect and (ii) the Coulomb barrier top effect. In order to investigate such effects in mirror nuclei, ^{11}Be and ^{11}N, we calculate the complex expectation values by using a new calculational method based on CSM [13]. In Sec. II, we describe the present method and model. In Sec. III, we explain the mechanisms of the differential energy shift. Results and discussions are given in Sec. IV, and summaries and conclusions are given in Sec. V.

II. METHOD AND MODEL

A. The complex scaling method

We describe a practical prescription concerning how to solve bound and resonance states by using CSM. In CSM, we define the following $U(\theta)$ transformation of the spatial coordinates and their conjugate momenta:

$$U(\theta): \quad \mathbf{r}\rightarrow \mathbf{r}\exp(i\theta), \quad \mathbf{p}\rightarrow \mathbf{p}\exp(-i\theta). \tag{1}$$

Here, θ is a scaling parameter of a real number. By using this transformation, we rewrite the Shrödinger equation $H\Phi = E\Phi$, as

$$H_\theta \Phi_\theta = E\Phi_\theta, \tag{2}$$

where $H_\theta = U(\theta)HU^{-1}(\theta)$ and $\Phi_\theta = U(\theta)\Phi$.

According to the ABC theorem [19], we can obtain the resonance energies (E_r) and widths (Γ) as complex energy eigenvalues ($E_r - i\Gamma/2$) of non-Hermitian H_θ with a complex scaled wave function Φ_θ. Resonant eigenvalues are complex numbers, and it should be independent of the scaling parameter θ $\{>\frac{1}{2}\tan[\Gamma/(2E_r)]\}$. It is also a very promising property of CSM that $H(\theta)$ gives the same eigenvalues (negative-real) for the bound states as those of the original (nonscaled) Hamiltonian, independently of θ. All other eigenvalues of H_θ—except for those of the bound and resonant solutions—depend on θ; this dependence is regularly proportional to $\exp(-2i\theta)$ on the complex-energy plane.

B. Complex expectation values

We now describe the complex expectation values of operators with the obtained complex scaled wave function. The complex expectation value has usually been calculated by using several methods, such as the convergent factor method or the analytical continuation method. However, in practical calculations, these methods have a numerical instability for resonance states with broad decay widths. On the other hand, as shown in Ref. [13], we can easily and accurately obtain complex expectation values that are the same as those for the bound states, because we only perform a simple integration of $(\Phi_\theta|\hat{O}_\theta|\Phi_\theta)$. Here, the round brackets represent the so-called *c* product [20]; $\Phi_\theta(k)$ and $\hat{O}_\theta$ are a scaled wave function and a scaled operator, respectively. This is mathematically connected to that of the convergent factor method by using the following relation [13,21]:

$$\langle\Phi|\hat{O}|\Phi\rangle \equiv \lim_{\alpha\rightarrow 0}\int d\boldsymbol{r}\Phi^*(-k^*,\boldsymbol{r})\hat{O}\Phi(k,\boldsymbol{r})e^{-\alpha r^2}$$
$$= (\Phi_\theta|\hat{O}_\theta|\Phi_\theta). \tag{3}$$

Since we do not have to use the limitation procedure ($\alpha \rightarrow 0$) as the convergent factor method, we can easily obtain the complex expectation values by calculating $(\Phi_\theta|\hat{O}_\theta|\Phi_\theta)$. Relation (3) holds when $\theta>\frac{1}{2}\tan[\Gamma/(2E_r)]$, which means a θ independence of $(\Phi_\theta|\hat{O}_\theta|\Phi_\theta)$, because of a constant value $\langle\Phi|\hat{O}|\Phi\rangle$ [13]. Numerically, this θ independence has been confirmed for some operators [13].

The complex expectation value of the Hamiltonian with the complex eigenfunction of bound and resonance states should be equal to the complex energy eigenvalue

$$(\Phi_\theta|H_\theta|\Phi_\theta) = E(\Phi_\theta|\Phi_\theta). \tag{4}$$

When the Hamiltonian is described as $H=T+V^N+V^C$, where T, V^N and V^C are the kinetic energy, the nuclear potential and the Coulomb potential operators, respectively, the sum of these complex expectation values is equal to the complex energy eigenvalue

$$E = (\Phi_\theta|T_\theta|\Phi_\theta) + (\Phi_\theta|V^N_\theta|\Phi_\theta) + (\Phi_\theta|V^C_\theta|\Phi_\theta). \tag{5}$$

Here, $(\Phi_\theta|\Phi_\theta)$ is normalized to unity by using the L^2 property of the complex scaled eigenfunction. In the above equation, the complex scaled eigenfunction and the complex scaled operators have a θ dependence, respectively. We may naively expect that each part of the expectation value has a θ dependence. However, as mentioned above in relation (3), $(\Phi_\theta|\hat{O}_\theta|\Phi_\theta)$ does not have any θ dependence. Therefore, we can uniquely divide the complex expectation value of the Hamiltonian into the kinetic energy and the potential energy parts, which are θ independent when $\theta>\frac{1}{2}\tan[\Gamma/(2E_r)]$. The physical meaning of a resonant quantity, such as the complex probability, the complex matrix element and the

complex expectation value are discussed by Berggren [22] in detail, where the real part is the mean value and the imaginary part is the ability to decay. We can then interpret the real part of the complex energy expectation value as a mean energy based on Berggren's picture.

C. Core+N model

We describe the present core+N Hamiltonian. The details are given in Refs. [24,7]. The Hamiltonian of the present core+N model is given as

$$H = T + V^N + V^C + V^P, \tag{6}$$

where T, V^N, and V^C are the kinetic energy, the nuclear potential and the Coulomb potential operators, respectively, and V^P is a so-called pseudopotential to project out the Pauli forbidden states [23]. As a core-N potential, we use a folding-type potential based on a nucleon-nucleon interaction, as discussed in Ref. [24]. Here, we assume that the core wave function has the ground configuration of the Harmonic oscillator shell model, as $(0s)^4(0p_{3/2})^2(0p_{3/2})^4$, with a size parameter of $b=1.63$ fm, which is discussed in Ref. [24].

In making the central potential $V^{\rm cnt}$ in V^N, we use an effective nucleon-nucleon interaction with a Gaussian form, as follows:

$$v(\boldsymbol{r}_i,\boldsymbol{r}_j) = \sum_n [W_n + B_n P_\sigma^{ij} - H_n P_\tau^{ij} - M_n P_\sigma^{ij} P_\tau^{ij}] v_n \times \exp[-\rho_n(\boldsymbol{r}_i - \boldsymbol{r}_j)^2], \tag{7}$$

where P_σ^{ij} and P_τ^{ij} are the spin and isospin exchange operators. In this calculation, we use the same parameters as those of MHN [25], which can well reproduce the spin-doublet partner of the ^{10}Li ground state [24]. Then, the central potential $V^{\rm cnt}$ is given as

$$V^{\rm cnt} = \sum_n \left(\frac{10}{9\xi_n/2+10}\right)^{3/2} \times \exp\left[-\frac{11\xi_n/2}{9\xi_n/2+10}\left(\sqrt{\frac{10}{11}}\frac{r}{b}\right)^2\right] v_n \times \Bigg[(10W_n + 5B_n - 6H_n - 3M_n) - (6W_n + 3B_n - 4H_n - 2M_n)\frac{5\xi_n}{9\xi_n/2+10} + (6W_n+3B_n)\frac{110(\xi_n)^2}{6(9\xi_n/2+10)^2}\left(\sqrt{\frac{10}{11}}\frac{r}{b}\right)^2\Bigg], \tag{8}$$

where ξ_n is given as $2\rho_n b^2$. Further, we introduce a δ parameter into the central potential in order to reproduce the experimental binding energy, where the midrange of the nucleon-nucleon interaction is changed as $(1+\delta)v_2$. The present δ value is -0.0062 for the p wave [24] and is 0.1252 for the s wave [7].

The spin-orbit potential V^{ls} in V^N of a density-derivative type is given as

$$V^{ls} = \frac{1}{2}V_0^{ls}\left[j(j+1) - l(l+1) - \frac{3}{4}\right]\frac{80}{27\sqrt{10\pi}b^3} \times \exp\left[-\frac{11}{9}\left(\sqrt{\frac{10}{11}}\frac{r}{b}\right)^2\right]\left[1 - \frac{44}{9}\left(\sqrt{\frac{10}{11}}\frac{r}{b}\right)^2\right]. \tag{9}$$

Here, the strength of the spin-orbit potential ($V^{ls} = 44.20$ MeV fm^3) is determined in ^{11}Be [24]. The folding-type Coulomb potential is given as

$$V^C = 6e^2\frac{1}{r}\mathrm{erf}(sr), \tag{10}$$

where s is $\sqrt{\frac{10}{9}1/b^2}$.

In order to remove the Pauli forbidden states for the valence nucleon, we apply the pseudopotential [23] as

$$V^P = \lambda[|0s_{1/2}\rangle\langle 0s_{1/2}| + |0p_{3/2}\rangle\langle 0p_{3/2}|]. \tag{11}$$

Here, $|0s_{1/2}\rangle$ and $|0p_{3/2}\rangle$ are the s and p waves for the core nucleus expressed by the harmonic-oscillator wave functions, which couple with the valence nucleon's spin 1/2. We use a large value, such as $\lambda = 10^4$ MeV, to push up the Pauli forbidden state.

III. THE s-WAVE HALO AND COULOMB BARRIER TOP EFFECTS

In this section, we discuss two effects: (i) the s-wave halo effect and (ii) the Coulomb barrier top effect in the s-p wave differential energy shift in mirror nuclei. Effect (i) is a revision of the Thomas-Ehrman effect, and effect (ii) is a complementary effect which becomes important in a loosely proton bound state measured from the Coulomb barrier top or, especially, in a proton unbound state. Here, it should be mentioned that we use the meaning of the Thomas-Ehrman effect in a narrow definition. The explanation given in this section is based on a simple picture in order to show their essence. A practical discussion for mirror nuclei (^{11}Be-^{11}N) is given in Sec. IV.

(i) *The s-wave halo effect*. Here, we reinterpret the Thomas-Ehrman effect as an s-wave halo effect. The Thomas-Ehrman shift has been observed as an differential energy shift related to the s wave between mirror states [8,9]. This energy shift has been explained as an effect mainly coming from the Coulomb energy difference for different particle orbits [11]. For weakly bound s states, it is known that the averaged Coulomb energy ($\langle\Psi_s|V^C|\Psi_s\rangle$) is reduced compared to other orbital states [11]. In the case of normal bound systems, since the spatial extent of nucleons is not so much different, we can expect almost the same averaged Coulomb energy. It would also be confirmed by seeing the symmetry of the isobaric analogue levels for normal nuclei. On the other hand, for a weakly bound system, the problem is why the remarkable averaged Coulomb energy difference arises. It would show a peculiarity for the wave function

(Ψ_s) of a weakly bound *s* state when the Coulomb potential (V^C) does not depend on the relative angular momenta.

Recently, for weakly bound systems, a peculiarity for the wave function of the weakly bound state is known. It is a so-called halo structure, which is explained by introducing spatially extended wave functions of the weakly binding valence nucleons around a core nucleus. Here, we use the meaning of the ''halo'' not only for the tail of the wave function, but also for the spatially extended property of the valence nucleons due to the weak binding. Especially for an *s*-wave neutron of the core+n system, it has been well investigated that the wave function is spatially extended than the other waves, even at the same binding energy. This is because the *s*-wave neutron does not have a centrifugal barrier which makes the amplitude of the tail part small.

We consider a mirror weakly bound system assuming that the core+n and core+p wave functions are not very much different. The wave function of low partial waves with weak binding is known to be spatially extended. Since the Coulomb interaction is dumped with an order of r^{-1}, it is expected that the Coulomb energy is reduced for such spatially extended states. Especially for the *s* state, investigations have shown that the spatial extent is larger than others due to no centrifugal potential. In other words, especially for the *s* state, the spatially extended halo wave function can reduce the Coulomb energy. It is noted that the present mechanism does not come from the difference between the core+n and core+p wave functions, but from the spatial extended property of the weakly bound *s* state compared to others due to no centrifugal potential.

Further, we comment on the Thomas-Ehrman effect in terms of a broad definition. As a higher order of the Thomas-Ehrman effect, we can consider an energy shift originating from the difference between the mirror core+N wave functions. The origin of the change from the core+n wave function to the core+p one mainly comes from the Coulomb barrier, because the core+n system does not have a potential barrier. The core+p wave function of the *s* state can be regarded as different in three parts from the core+n one: (i) inner, (ii) around and (iii) outer region of the Coulomb barrier. If the proton binding is strong enough measured from the barrier top, the core+p wave function for the *s* state shrinks within the inner region of the potential barrier, and the spatial extent becomes near to those of other orbital states. In other words, this shrunken wave function of the *s* state recovers the mirror symmetry of the spectrum because of a similar spatial extent compared to other orbital states. On the other hand, if the valence proton is loose or not binding, measured from the (i) barrier top, since it can pass through the barrier, (ii) the proton around the barrier, and (iii) that outer region cannot be neglected. In the next subsection, we discuss such a case.

When the *s*-wave valence proton is assumed to be more spatially extended than others, the averaged Coulomb energy becomes small in comparison with others. We also show that the Coulomb energy calculated with the wave function of the halo *s* state is smaller than that of the *p* state discussed in Sec. IV. The reduction of the Coulomb energy for the halo orbit seems to give an explanation of the Thomas-Ehrman effect [11]: if the binding of the *s* wave is weaker, the averaged Coulomb energy is smaller. We can then reinterpret the Thomas-Ehrman effect as one of the halo effects. Once this interpretation is shown to be valid, we have had ''another proof of the halo'' for this past half century in addition to the observation of the large matter radius in the drip-line nuclei [26]. Of course, the observed Thomas-Ehrman shift also includes an effect from the symmetry breaking of the mirror wave functions, if it is possible. We next discuss a remarkable symmetry breaking originating from the Coulomb barrier top.

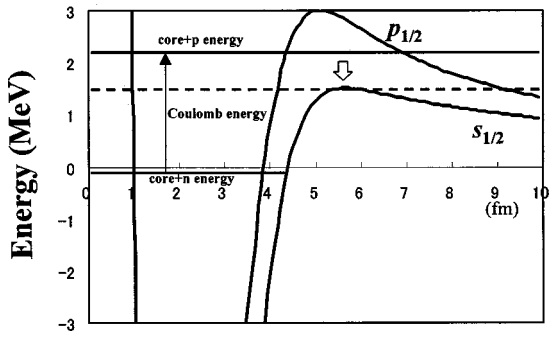

FIG. 2. Schematic figure of difference between the *s* and *p* states in the core+p system. The solid line is an estimated energy and the dotted line is the Coulomb barrier top energy. The potentials for the *s* and *p* states are also shown.

(ii) *The Coulomb barrier top effect.* We discuss the Coulomb barrier top effect. This effect becomes important in a proton loosely bound state measured from the Coulomb barrier top, or especially in a proton unbound state. In the energy region just below the Coulomb barrier top of the core+p system (proton loosely bound one), the valence proton can tunnel the barrier because of a tunneling effect. In the energy region above it (proton unbound one), a valence proton easily passes through the outer region of the barrier. In the outer region of the barrier, the kinetic and potential energies are smaller than those in the inner region. Hence, an additional energy shift is expected due to energy reduction when the core+p wave function is changed from the mirror one. For other waves, since they are regarded as being bound states measured from their orbital barrier top due to an additional centrifugal potential, it is expected that the spatial extent between mirror wave functions is not so much different. Off course, when the binding energy measured from the barrier top becomes small enough, the barrier top effect also arises for other waves.

We explain the above mechanism using a schematic model (see Fig. 2). Typical potentials ($Z=6$) of *s* and *p* waves are given in Fig. 2. For the *p*-wave potential, the centrifugal one is also included, though the *s* wave has only a Coulomb barrier. The Coulomb energy is estimated as $Ze^2/r=6\times1.44/4=2.16$ MeV in the case of a typical core-N distance of $r=4$ fm. If the binding energy of the core+n system for both the *s* and *p* states is assumed to be near the threshold energy (~0 MeV), the energy of the mirror core+p system can be estimated by using the Coulomb energy. The solid line around 2.1 MeV shows such an energy.

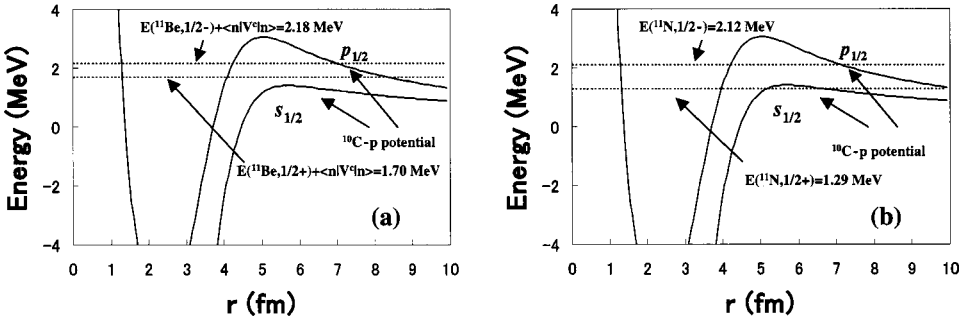

FIG. 3. (a) Estimated energies and (b) resonance energies (the real parts of true energy eigenvalues) for the *s* and *p* states of ^{11}N with the ^{10}C-*p* potentials.

We can see that it is above the barrier top energy of the *s* wave (dashed line), though the estimated energy is below that of the *p* wave due to the Coulomb potential plus the centrifugal one. In this situation above the barrier top energy region, the *s*-wave proton cannot be regarded as being a confined state within the inner region of the barrier. This is because the proton can easily pass through the barrier top to the outer region. Hence, it is considered that the core-*p* wave function can become spatially more extended than the core-*n* one. When the ratio of the proton in the outer region becomes large, the total energy can reduce because the spatially extended wave function can have a small energy. This is because the kinetic energy and the Coulomb potential terms become small, though it is partly compensated by the attractive nuclear potential reduction.

Since this explanation is based on a simple estimation, it should be confirmed by solving the eigenvalue problem for the actual Hamiltonian. In the next section, we show them (e.g., the kinetic energy reduction) in typical mirror pair nuclei, ^{11}Be-^{11}N. Concerning the experimental situation of this pair, the *s*-wave resonance energy in ^{11}N is observed at $E_r = 1.3$ MeV [2]. It is very close to the Coulomb barrier top energy (~ 1.3 MeV) for the ^{10}C-*p* system, which is just the situation of the Coulomb barrier top effect.

IV. RESULTS

First, we show the *s*-wave halo effect in the *s*-*p* wave differential energy shift between *s* and *p* states for mirror nuclei ^{11}Be and ^{11}N. This effect shows a spatially extended property of the *s* state compared to others. The energy shift of this effect is estimated by assuming the same core$+N$ wave functions. By using the wave function $\Psi(n)$ of ^{11}Be, which is obtained with the Hamiltonian given in Sec. II C, we calculate the Coulomb energy $\langle\Psi(n)|V^C|\Psi(n)\rangle$. Here, we note that the wave function is the same as that in the previous calculations [24,7]. The value for the *s* state is 2.20 MeV, and that for the *p* state is 2.36 MeV. The *s*-wave Coulomb energy is smaller than the *p*-wave one, as expected. The Coulomb energy difference $2.36-2.20=0.16$ MeV is a reasonable value compared with the usual Thomas-Ehrman shift one. When the halo tail reduces in the ^{10}C$+p$ system, though we assume the same halo wave function in the present estimation, the *s*-wave energy shift would become a smaller value than 0.16 MeV, as mentioned in Sec. III. However, the experimental energy shift (0.42 MeV) is much larger.

We next show that the above estimation of the *s*-wave energy shift is not sufficient, and a further effect may arise: the Coulomb barrier top effect. When the mirror core$+N$ wave functions are not very different, the energy of ^{11}N measured from the ^{10}C-*p* threshold is estimated by using the energy of ^{11}Be and the above Coulomb energy as $E = E(^{11}\mathrm{Be}) + \langle\Psi(n)|V^C|\Psi(n)\rangle$. By using the calculated energy of ^{11}Be, the energy of ^{11}N is estimated to be $E = E(^{11}\mathrm{Be}) + \langle V^C\rangle = -0.50 + 2.20 = 1.70$ MeV for the *s* state and $E = -0.18 + 2.36 = 2.18$ MeV for the *p* state. In Fig. 3(a), we show these estimated energies (dotted lines) with ^{10}C-*p* potentials. As shown in Fig. 3(a), the estimated energy level is above the Coulomb barrier top for the *s* state, while it is below the barrier top for the *p* state. Then, for the *s* state, the large deviation of the core-*p* wave function from the core-*n* one is expected, because the valence proton cannot be confined in the inner region of the barrier. In other words, the actual energy eigenvalue may deviate from the estimated energy due to a change of the wave function.

In Fig. 3(b), we show the actual energy eigenvalues (dotted lines) solved with an accurate boundary condition in the asymptotic region. The real part of the obtained energy eigenvalue (resonance energy $E_r = 1.29$ MeV) for the *s* state is very close to the Coulomb barrier top energy different from the estimated energy ($E = 1.70$ MeV) in Fig. 3(a). Since we assume in the estimation that the ^{11}Be wave function is the same as the ^{11}N one, this *s*-wave energy deviation from the estimation is considered to come from the difference between the core-*n* and core-*p* wave functions. On the other hand, the resonance energy ($E_r = 2.12$ MeV) of the *p* state is almost the same as the estimated energy ($E = 2.18$ MeV) in Fig. 3(a). It is easily understood that the estimated energy for the *p* state is below the barrier top, which means that the main part of the core-*p* wave function is not different from the core-*n* one, though there is a slight deviation coming from the penetration of the tail part and confinement due to the barrier.

The remaining problem is to investigate the origin of the additional energy shift as seen from the resonance energy of the *s* state in Fig. 3(b). In order to study them, we calculated complex expectation values of the kinetic and the potential energy operators for the *s* and *p* states in ^{11}Be and ^{11}N, as shown in Table I. The Coulomb energy in parentheses for ^{11}Be is the estimated value given in the above discussion. As shown in Table I, for ^{11}N, the real part of the calculated complex expectation values for the kinetic energy operator and the nuclear potential operator are greatly reduced com-

TABLE I. Calculated complex expectation values for each operator with complex energy eigenvalues for the *s* and *p* states in ^{11}Be and ^{11}N. Third line is energy eigenvalue, the fourth is the complex expectation value of the kinetic energy, the fifth is that of the nuclear potential and the sixth is that of the Coulomb potential. The last line is that of the Hamiltonian and it is the same value of the energy eigenvalue, as expected. The Coulomb ones for ^{11}Be are estimated values for ^{11}N by using the ^{11}Be wave function.

	^{11}Be (MeV)		^{11}N (MeV)	
	s state	*p* state	*s* state	*p* state
E	-0.503	-0.183	$1.29-i0.70$	$2.12-i0.47$
$\langle T\rangle$	11.221	8.008	$4.39-i8.57$	$6.80-i3.93$
$\langle V^N\rangle$	-11.724	-8.191	$-5.02+i8.95$	$-7.13+i4.12$
$\langle V^C\rangle$	(2.20)	(2.36)	$1.93-i1.07$	$2.46-i0.66$
$\langle H\rangle$	-0.503	-0.183	$1.29-i0.70$	$2.12-i0.47$

pared to ^{11}Be. For example, the kinetic energy of ^{11}Be for the *s* state is $\langle T\rangle = 11.2$ MeV, and that of ^{11}N is $\mathrm{Re}\langle T\rangle = 4.4$ MeV, where Re means the real part. This shows the large kinetic energy reduction as $\delta\langle T\rangle = 11.2-4.4=6.8$ MeV. Since the spatially extended wave function reduces the kinetic energy, we can understand that the ^{11}N wave function of the *s* state is spatially extended. Furthermore, it is also worth seeing the case of the *p* state, where the energy reduction also arises from ^{11}Be to ^{11}N, even though it is not so much larger than the *s* state. Since the *p* state in ^{11}N is weakly bound from the (Coulomb+centrifugal) barrier top, the resonant property near the barrier top is also important.

In Table II, we show the energy differences between the *s* and *p* states by using the values given in Table I. The energy difference, $\Delta E_{s\text{-}p}$, is calculated by using the real part of the complex energy as $\mathrm{Re}\langle E_p\rangle - \mathrm{Re}\langle E_s\rangle$. The kinetic and the nuclear potential energy difference $\Delta(\langle T\rangle + \langle V^N\rangle)_{s\text{-}p}$, and the Coulomb energy difference $\Delta(\langle V^C\rangle)_{s\text{-}p}$, are also calculated in a similar way. The total energy shift is $\delta E = 0.834 - 0.320 = 0.514$ MeV. Since the Coulomb energy difference in ^{11}N is 0.526 MeV, as shown in Table II, it is very close to the total energy shift $\delta E = 0.514$ MeV. On the other hand, the sum of the kinetic energy difference and the nuclear potential differences in ^{11}Be and ^{11}N are almost the same, 0.308 MeV for ^{11}Be and 0.320 MeV for ^{11}N, which seems to cancel each other as $0.308-0.320\sim 0$ MeV. Hence, for the mirror pair ^{11}Be and ^{11}N, even though both reductions between the *s* and *p* wave of the kinetic and the nuclear potential energies are large, they cancel each other. However, the Coulomb energy reduction between the wave functions of the mirror nuclei remain. Our calculated energy (0.53 MeV) is three-times larger than an estimated energy (0.16 MeV) of assuming the same wave functions between the mirror nuclei. This large Coulomb energy reduction in addition to the energy reduction for each operator can be understood by considering the spatially extended core-*p* wave function.

TABLE II. Energy differences between the *s* and *p* states in ^{11}Be and ^{11}N. These values are obtained by using the real part of the complex expectation values given in Table I. Here, the difference is described as, $\Delta O_{s\text{-}p} = \mathrm{Re}\langle O_p\rangle - \mathrm{Re}\langle O_s\rangle$. For example, the energy difference for ^{11}N is calculated as $\Delta E_{s\text{-}p} = \mathrm{Re}\langle E_p\rangle - \mathrm{Re}\langle E_s\rangle = 2.12-1.29=0.83$ MeV.

	^{11}Be (MeV)	^{11}N (MeV)
$\Delta E_{s\text{-}p}$	0.320	0.834
$\Delta(\langle T\rangle + \langle V^N\rangle)_{s\text{-}p}$	0.320	0.308
$\Delta(\langle V^C\rangle)_{s\text{-}p}$	(0.155)	0.526

Finally, as a comment, we discussed the extreme case of the loosely bound states for the *s* and *d* waves in the previous paper [16]. In such a case, we show that the real part of $\langle T\rangle + \langle V^N\rangle$ for the *s* state in the core+*p* system is very different from that of the core+*n* system, while it is not so different for the *d* state. In the present ^{11}Be-^{11}N case, such a large difference does not occur, because the present binding energy of the *s* state (0.5 MeV) is less than that in the previous calculation (0.1 MeV), and the *p*-wave barrier is smaller than the *d*-wave one.

V. SUMMARIES AND CONCLUSIONS

In summary, we investigated the *s*-wave halo effect and the Coulomb barrier top effect for the *s*-*p* wave differential energy shift (Thomas-Ehrman shift) in ^{11}Be-^{11}N. In this paper, we calculated the complex energy expectation values using the new method of CSM, which was proposed by Homma, Myo, and Kato [13].

For the ^{10}C+*p* system, by assuming a spatially extended wave function of the halo which is the same as that of ^{11}Be, we can understand that the *s*-wave halo reduces the Coulomb energy in the core+*p* system. However, such a Coulomb energy shift (0.16 MeV) is rather smaller than the experimental *s* wave energy shift (0.42 MeV) in ^{11}N. If there is such a large Coulomb energy shift of the experimental one, the wave function of the *s*-wave would be spatially more extended. On the other hand, the experimental and calculated resonance energy are very close to the Coulomb barrier top energy. Around the barrier top energy region, the valence proton easily passes through the barrier to the outer region. Then, another effect of the spatially extended valence proton in the resonance state arises.

In order to see the spatially extended property, we considered the energy reductions for each operators by using the solution of the eigenvalue problem. The result shows a large energy reduction (e.g., kinetic energy reduction). Since the kinetic energy and the nuclear potential energy reductions are of the same order, they cancel each other, but the Coulomb energy reduction remains. In other words, the repulsive kinetic energy and the Coulomb energy reduce, though it is compensated by the attractive nuclear potential energy reduction. The remaining energy reduction which is not canceled is the origin of the energy shift. This remaining energy reduction (0.51 MeV) explains the experimental energy shift (0.42 MeV). Here, we note that the calculated results should be slightly larger than the experimental one, because the experimental $1/2+$ state is expected to have a *d*-wave minor component, which would confine the valence proton due to the *d*-wave barrier.

Although the present effects were investigated within a simple core-N model, it would also be important for studies of more complicated systems. For example, we can suggest that a study of the anomalous energy shift in isobaric analogue states, such as ^{11}Li (^{9}Li$+n+n$)-^{11}Be* (^{9}Li$+p+n$), is an interesting problem. The energy shifts related to the s wave in unstable nuclei are considered to be related to the halo structure, as discussed in the present paper. Therefore, it is expected to give insight to the halo structure from another point of view. In the future, we will systematically investigate the energy shift in unstable nuclei.

ACKNOWLEDGMENTS

The author would like to thank Professor K. Katō and Professor K. Ikeda for various discussions and encouragements, and Professor I. Tanihata, Professor H. Nakada, Dr. H. Masui, and Dr. N. Itagaki for helpful discussions.

[1] *Proceedings of the 5th ISPU in Niigata* [Nucl. Phys. **A588**, 1 (1995)]; *Proceedings of the 4th International Conference on Radioactive Nuclear Beam, Omiya* [*ibid.* **A616**, 1 (1997)].

[2] L. Axelsson, M.J.G. Borge, S. Fayans, V.Z. Goldberg, S. Grévy, D. Guillemaud-Mueller, B. Jonson, K.-M. Källman, T. Lönnroth, M. Lewitowicz, P. Manngard, K. Markenroth, I. Martel, A.C. Mueller, I. Mukha, T. Nilsson, G. Nyman, N.A. Orr, K. Riisager, G.V. Rogatchev, M.-G. Saint-Laurent, I.N. Serikov, O. Sorlin, O. Tengblad, F. Wenander, J.S. Winfield, and R. Wolski, Phys. Rev. C **54**, R1511 (1996).

[3] V. Guimarães, S. Kubono, M. Hosaka, N. Ikeda, S.C.Jeong;, I. Katayama, T. Miyachi, T. Nomura, M.H. Tanaka, Y. Fuchi, H. Kawashima, S. Ohkawa, S. Kato, H. Toyokawa, C.C. Yun, T. Niizeki, K. Ito, T. Kishida, T. Kubo, Y. Pu, M. Ohura, H. Orihara, T. Terakawa, S. Hamada, M. Hirai, and H. Miyatake, Nucl. Phys. **A588**, 161c (1995).

[4] H.T. Fortune, D. Koltenuk, and C.K. Lau, Phys. Rev. C **51**, 3023 (1995).

[5] F.C. Barker, Phys. Rev. C **53**, 1449 (1996).

[6] P. Descouvemont, Nucl. Phys. **A615**, 261 (1997).

[7] S. Aoyama, N. Itagaki, K. Katō, and K. Ikeda, Phys. Rev. C **57**, 975 (1998).

[8] J.B. Ehrman, Phys. Rev. **81**, 412 (1951).

[9] R.G. Thomas, Phys. Rev. **88**, 1109 (1952).

[10] F. Ajzenberg-Selove, Nucl. Phys. **A490**, 1 (1988); **A433**, 1 (1985).

[11] A. Bohr and B. Mottelson, *Nuclear Structure* (Benjamin, New York, 1969), Vol. 1.

[12] E. Comay, I. Kelson, and A. Zidon, Phys. Lett. B **210**, 31 (1988).

[13] M. Homma, T. Myo, and K. Katō, Prog. Theor. Phys. **97**, 561 (1997); T. Myo and K. Katō, *ibid.* **98**, 1275 (1998).

[14] S. Aoyama, Phys. Rev. C **59**, 531 (1999); S. Aoyama, K. Katō, and K. Ikeda, Phys. Lett. B **414**, 13 (1997); S. Aoyama, K. Katō, and K. Ikeda, Phys. Rev. C **55**, 2379 (1997).

[15] A. Csótó, Phys. Rev. C **49**, 3035 (1994).

[16] S. Aoyama, K. Katō and K. Ikeda, Prog. Theor. Phys. **99**, 623 (1998).

[17] K. Ogawa, H. Nakada, S. Hino, and R. Motegi, Phys. Lett. B **464**, 157 (1999).

[18] A. Muta and T. Otsuka (private comunication).

[19] J. Aguilar and J.M. Combes, Commun. Math. Phys. **22**, 269 (1971); E. Balslev, and J.M. Combes, *ibid.* **22**, 280 (1971).

[20] N. Moiseyev, P.R. Certain, and F. Weinhold, Mol. Phys. **36**, 1613 (1978).

[21] B. Gyarmati, A.T. Kruppa, and K.F. Pal, Phys. Rev. A **41**, 3469 (1990).

[22] T. Berggren, Phys. Lett. **33B**, 547 (1970); Phys. Lett. B **373**, 1 (1996).

[23] V.I. Kukulin, V.M. Krasnopol'sky, V.T. Voronchev, and P.B. Sazonov, Nucl. Phys. **A453**, 365 (1986).

[24] K. Katō and K. Ikeda, Prog. Theor. Phys. **89**, 623 (1993).

[25] F. Tanabe, A. Tohsaki, and R. Tamagaki, Prog. Theor. Phys. **53**, 677 (1975).

[26] I. Tanihata, H. Hamagaki, O. Hashimoto, S. Nagamiya, Y. Shida, N. Yoshikawa, O. Yamakawa, K. Sugimoto, T. Kobayashi, D.E. Greiner, N. Takahashi, and Y. Nojiri, Phys. Lett. **160B**, 380 (1985).